Plant Molecular Biology (2006) 61:329–344
DOI 10.1007/s11103-006-0015-x

Subtractive cDNA libraries identify differentially expressed genes in dormant and growing buds of leafy spurge (*Euphorbia esula*)

Ying Jia[1], James V. Anderson[2], David P. Horvath[2], Yong-Qiang Gu[3], Rodney G. Lym[1] and Wun S. Chao[2,*]
[1]*Department of Plant Sciences, North Dakota State University, Fargo ND 58105, USA;* [2]*Plant Science Research, USDA-Agricultural Research Service, 1605 Albrecht Blvd., Fargo ND 58105-5674, USA (*author for correspondence; e-mail chaow@fargo.ars.usda.gov);* [3]*Western Regional Research Center, USDA-ARS, Albany CA 94710, USA*

Received 27 September 2005; accepted in revised form 23 January 2006

Key words: dormancy, leafy spurge, subtractive hybridization

Abstract

Two subtractive cDNA libraries were developed to study genes associated with bud dormancy (reverse library) and initiation of shoot growth (forward library) in leafy spurge. To identify unique sequences represented in each library, 15744 clones were screened to reduce the level of redundancy within both libraries. A total of 516 unique sequences were obtained from 2304 minimally redundant clones. Radioactive probes developed from RNAs extracted from crown buds of either intact (para-dormant control) or a series of growth-induced (2 h, 2, and 4 d after decapitation) plants were used to identify differentially expressed genes by macroarray analysis. Semi-quantitative RT-PCR was used to confirm results obtained by macroarray analysis and to determine the expression profiles for other transcripts identified within the subtractive libraries. Selected clones were also used to examine gene expression in crown buds after growth induction and/or during normal seasonal growth. In this study, four distinct patterns of gene expression were observed during the transition from para-dormancy to growth-induction. Many of the differentially regulated genes identified have unknown or hypothetical functions while others are known to play important roles in molecular functions. Gene ontology analysis identified a greater proportion of genes involved with catalytic activity in the forward library while the reverse library had a greater proportion of genes involved in DNA/RNA binding.

Introduction

Leafy spurge (*Euphorbia esula* L.) is a deep-rooted perennial weed that infests range and recreational lands in the northern Great Plains of the United State and Canada. Vegetative propagation through the growth of underground adventitious buds on the root and crown (i.e. root and crown buds) is the primary means of reproduction and maintenance of its perennial nature (Coupland *et al.*, 1955). These buds undergo well-defined phases of dormancy throughout the year (for more information about seasonal changes in dormancy status of leafy spurge, see Horvath *et al.*, 2003; Anderson *et al.*, 2005), but will usually develop new shoots if top growth is damaged or separated from the roots under environmental conditions conducive to growth. Dormancy-imposed growth arrest is one of the key characteristics that make leafy spurge persistent and difficult to control (CAB, 2004).

Phytohormones, nutrients, water status, flowering, day-length, temperature, and post-senescence affect crown and root bud dormancy (McIntyre, 1972; Nissen and Foley, 1987a, 1987b;

Harvey and Nowierski, 1988; CAB, 2004; Anderson *et al*., 2005). Three phases of dormancy, para-, endo-, and eco-dormancy, were observed during the seasonal development of leafy spurge (Anderson *et al*., 2005; Chao *et al*., 2006). Para-dormancy, also called correlative inhibition, controls bud growth during the growing season. Two separate signals, one from the mature leaves and one from the meristems (apical or axillary buds), cause growth arrest (Horvath, 1998; 1999). Although either leaves or growing axillary buds was sufficient to inhibit root bud growth, the leaf-derived signal required photosynthesis for its production or transport, whereas no photosynthesis was required for the signal from growing axillary buds. Current results suggest that the leaf-derived signal is responsible for inhibiting the G_1/S-phase transition and may involve sugar perception (Horvath *et al*., 2002; Chao *et al*., 2006). The meristem-derived signal requires polar auxin transport, and is responsible for the inhibition of cell division post S-phase (Horvath *et al*., 2002).

Crown and root buds develop endo-dormancy (also called innate inhibition) in the fall. During endo-dormancy, bud growth is inhibited by internal physiological factors that may be associated with flowering, temperature, change of day-length, and post-senescence. As in many perennials, sufficient chilling breaks endo-dormancy in leafy spurge buds (Harvey and Nowierski, 1988; Nissen and Foley, 1987a; Horvath *et al*., 2003; Anderson *et al*., 2005; Chao *et al*., 2006). During over-wintering, bud growth is inhibited by surrounding cold temperature. This type of growth arrest is more commonly referred to as eco-dormancy.

Considerable effort has been directed towards understanding the mechanism of root bud dormancy; however, most work has been done at the physiological level and is mostly descriptive (Anderson *et al*., 2001). Molecular analyses are thus needed to identify and clone genes, to investigate gene functions and regulation, and to determine mechanisms that regulate bud dormancy and growth. Currently, several key developmental and cell cycle regulatory genes have been cloned and characterized (Anderson and Horvath, 2001; Horvath and Anderson, 2002; Horvath *et al*., 2002, 2005). These genes are useful since they could serve as markers for dormancy break and bud growth, but genes that are directly involved in the dormancy-related process have not been identified from leafy spurge. In other plant species (i.e. Johnsongrass, populus, potato, etc.), progress has been made to identify markers for quantitative trait loci (QTL) that are associated with dormancy in vegetative propagules (Freyre *et al*., 1994; Paterson *et al*., 1995; van den Berg *et al*., 1996; Šimko *et al*., 1997; Frewen *et al*., 2000). Some of the QTLs are associated with abscisic acid content (Šimko *et al*., 1997) or coincide with genes involved in abscisic acid signaling and photoperiod perception (Frewen *et al*., 2000). QTL analysis is not suitable for leafy spurge because of poorly defined genetics and lack of linkage or genetic maps.

Here we describe a genomics approach to identify and clone additional genes associated with dormancy and growth in the root and crown buds of leafy spurge based on subtractive hybridization, macroarray analysis, and RT-PCR. Subtractive hybridization allows comparisons between two populations of mRNA and identifies genes that are differentially expressed in the two populations. This technique has been widely used to isolate a large number of differentially expressed genes (Diatchenko *et al*., 1996; Bassani *et al*., 2004; Zheng *et al*., 2004). A forward (genes preferentially expressed in growing buds) and a reverse (genes preferentially expressed in dormant buds) subtractive cDNA library were generated. After library screening, 516 unique sequences were obtained. Their expression during dormancy and growth were examined and reported.

Materials and methods

Plant materials and RNA preparation

Greenhouse-grown leafy spurge (*Euphorbia esula* L.) was started as shoot cuttings from Biotype 1984-ND-001 and maintained by clonal propagation. Shoot cuttings from greenhouse-grown plants were placed in Sunshine #1 potting mix (Fisons Horticulture Inc., 110th Ave. N.E., Suite 490, Bellevue, WA) inside 4×21 cm Ray Leach Cone-tainers (SC-10 super cell, Stuewe and Sons Inc., Corvallis, OR) and grown in a greenhouse under a 16:8 h day:night photoperiod

cycle at 28 ± 4 °C for 3–4 mo. Root buds collected in 2002 were used to isolate RNA for construction of subtractive cDNA libraries. Growth-induced buds were collected every 12 h for 3 d after plants were decapitated. Control (dormant) buds from the intact plants were harvested at the same time points as induced buds. To minimize background problems caused by circadian rhythm, induced buds, as well as control buds, harvested from six different time points were pooled and used to extract total RNA using the method described by Chang et al. (1993).

Gene expression is very similar between crown and root buds (unpublished observations). For the ease of harvesting bud samples, we thus used crown buds to monitor expression analyses. Three biological sets of crown buds were harvested from greenhouse-grown plants in April 2003, November 2003, and November 2004. Control buds were collected from the intact plants (0 h), and induced buds were collected over a series of time points, 2, 4, 8, 16 h, 1, 2, 3, 4, 5 d after plants were decapitated. RT-PCR was done using at least two sets of replicates.

Field-grown leafy spurge plants were established by transplanting a portion of the greenhouse population to a field plot in 1998. Two sets of crown buds were harvested from this plot. One set was harvested monthly from July through Feb. of 2002–2003, and a replicate set was harvested in corresponding months of 2003–2004. These buds were used to study seasonal effects on gene expression using RT-PCR.

Subtractive library construction, differential screening, large-scale library screening, and sequencing

Two PCR-Select subtractive libraries were constructed by Clontech (Palo Alto, CA) following the instruction manual of Clontech PCR-Select cDNA Subtraction Kit. The forward library (RT) contains genes preferentially expressed in growing buds and the reverse library (RD) contains genes preferentially expressed in dormant buds. Briefly, for the RT library, 'driver' cDNA was synthesized from the mRNA isolated from root buds of intact plants, and 'tester' cDNA was produced from mRNA isolated from the pooled time points after growth induction by decapitation of the aerial tissue down to the crown of the root. The RD library was made by reversing tester and driver cDNAs. The poly A^+ RNA fractions from intact and decapitated plant samples were isolated by two rounds of poly A^+ selection on oligo(dT)-latex beads using the Clontech Nucleotrap mRNA Midi Kit. Subtractive hybridization was performed with 1 (tester):30 (driver) ratio in both directions, and the subtracted cDNA pool was amplified by PCR. Purified secondary PCR-amplified product (40 ng) was cloned into the pAtlas vector (PUC base vector). The ratio of white to blue colonies for both libraries was about 2 to 1, and 80% of white colonies contained plasmid with insert. Each library contained about 7000 independent cDNA clones when it was originally made. Differential screening was performed according to Clontech's PCR-Select Differential Screening Kit User manual (K 1808-1).

For large-scale library screening, 15744 clones were picked and grown in 384-well microtiter plates in LB containing 10% glycerol and 75 mg/l ampicillin. These clones (8064 clones from the RD library and 7680 clones from the RT library) were then spotted onto a 23×23 cm size membrane using Q-Bot (Genetix USA Inc, Boston, MA). Membranes were hybridized with ^{32}P-labeled probes made from eight groups of redundant clones (1–20 independent clones were combined as a group). A Hybsweeper computer program was used to count hybridized clones (Lazo *et al*., 2005). Sequencing of 2304 clones was performed by Agencourt Bioscience Corp. (Beverly, MA) and the Eastern Regional Research Center, Nucleic Acid Facility (Wyndmoor, PA). Contig and sequence analysis were carried out using the Lasergene 6.0 sequence analysis software (DNASTAR, Inc., Madison, WI).

cDNA macroarray preparation and analysis

The inserts of 516 unique sequences were amplified using a forward (5′-TCGAGCGGCCGCCCGGG CAGGT-3′) and a reverse (5′-AGCGTGGTC GCGGCCGAGGT-3′) primer. Reactions were done using 1 μl (1–2 ng) of template DNA in a 100 μl PCR mixture containing 10 μl of 10× PCR buffer, 2.4 μl of 10 mM nucleotide mix, 1.2 μl of each primer (20 pmol), 0.5 μl (2.5 U) pfu Ultra Hotstart High-Fidelity DNA polymerse (Stratagene, La Jolla, CA) and 83.7 μl sterile

water. PCR was performed on a RoboCycler Gradient 96 (Stratagene) with an initial denaturation step of 30 s at 94 °C, followed by 35 cycles of 50 s at 94 °C, 1 min at 45 °C, and 2 min at 72 °C. PCR products were purified using 96-well multiscreen filter plates (Millipore, Billerica, MA). PCR product (5 μl) was run on a 1% agarose gel to confirm amplification quality and quantity. PCR products < 100 ng/μl were re-amplified. PCR products were transfer to 384-well plates and spotted onto Hybond N^+ membrane (Amersham Biosciences, Piscataway, NJ) in duplicate using a 384 pin Multi-blot Replicator (V&P Scientific, Inc, San Diego, CA). The DNA-spotted membrane was denatured and neutralized according manufacture's specification for Hybond-N (Amersham Biosciences), dried at room temperature overnight, and stored at −20 °C for future use. Labeling was performed with a Strip-EZ^{TM}RT kit (Ambion, Inc., Austin, TX). Total RNA (2 μg) was reverse transcribed in the presence of [α-^{32}P]dATP with MMLV reverse transcriptase and oligo dT. ^{32}P-labeled cDNA probes were purified in a 10 ml Sepharose G-50 column based on the method described for a Sepharose CL-4B column (Sambrook *et al*., 1989). Hybridization, membrane washes, and probe digestion were performed as described by the instruction manual of the Strip-EZ^{TM}RT kit. The resulting arrays were scanned and recorded with a Parkard Instantimager (Packard Instrument Co. Downers Grove, IL.).

As a vast fraction of the clones did not appear to be differentially regulated, and since no known constitutively expressed genes were available for use as controls, global mean normalization was applied to scale all the test samples (2 h, 2, and 4 d) to have an identical average intensity with the control sample (0 h) (Sebastiani *et al*., 2003). Briefly, the average of absolute intensity from spots of control sample (represented as mean *C*) and averages of absolute intensity from spots of each time point of the induced samples (represented as mean *T*) were calculated. Values of each spot for a given time point were normalized to the 0 h average by multiplying the ratio of mean *C* to mean *T* (mean *C*/mean *T*). The ratio of the given induced time point verses the 0 h normalized hybridization intensities for each spot was calculated, and the fold induction or inhibition of expression for each gene verses the 0 h control was determined. The $\log_2$ converted average fold induction of replicate samples were used for cluster analysis.

Semi-quantitive RT-PCR

Total RNA was DNase (Invitrogen) treated and then reverse transcription was performed using a SuperScript First-Strand Synthesis Kit (Invitrogen) to produce total cDNA from each sample. For PCR reactions, total cDNA samples were diluted to 25 ng/μl, and 1 μl total cDNA was added to a 25 μl PCR reaction mixture containing 2.5 μl of 10× PCR buffer, 0.75 μl of 25 mM $MgCl_2$, 0.6 μl of 10 mM dNTPs, 0.5 μl of each primer (20 pmol), and 0.1 μl (5 U/μl) of platinum *Taq* DNA polymerase (Invitrogen). Thermal cycling was performed on a RoboCycler Gradient 96 (Stratagene) with an initial denaturation step of 2 min at 95 °C, followed by 18–35 cycles of 50 s at 94 °C, 1 min at various annealing temperatures according to the Tm of the primers, and 1 min at 72 °C. PCR reactions were electrophoresed on 1% agarose gels. Primers were designed using Lasergene sequence analysis software (DNASTAR, Inc). To each of these unique sequences, different annealing temperatures and cycles were examined to obtain a linear range of amplification before performing PCR with at least two sets of biological replicates. Different primers and PCR conditions are listed in Supplementary data 1. DNA bands on ethidium bromide stained gels were quantitated using a Fluor-S MultiImager and Quantity One 4.0 (BioRad, Hercules, CA).

Results

Differential screening, screening for non-redundant clones, and sequencing

Differential screening was performed initially using RT or RD cDNA probes to 1200 randomly selected clones from the RT and RD cDNA libraries (600 from the RT and 600 from the RD library); a method commonly applied for this type of work (Clontech, User Manual PT3138-1). The RT probes were made from the same subtracted cDNA used to generate the RT cDNA library and the RD probes were made from the same subtracted cDNA used to generate the RD library.

This approach should have increased the potential of detecting low-abundance, differentially regulated genes. We sequenced all the clones (214 clones from the RT library and 102 clones from the RD library) that showed a 2-fold difference in gene expression after differential screening analyses. Sequencing results only identified 25 unique sequences (Table 1, represented by * plus those listed in the footnotes at the bottom of the table) from the RD library and 17 unique sequences (Table 2, represented by * plus those listed in the footnotes at the bottom of the table) from the RT library due to high redundancy among these genes.

Differential screening indicated that there was fairly high redundancy in both subtractive libraries. A putative senescence-associated protein appeared 129 times in the RT library and a 5S ribosomal RNA appeared 48 times in the RD library. High redundancy was further revealed after randomly sequencing 100 clones from each cDNA library. The three most redundant sequences were senescence-associated protein (20%) from the RT library, a hypothetical protein (12.5%) from the RD library and lysine-ketoglutarate reductase (9.4%) from the RT library. Other redundant clones contained between 2 and 5 overlapping sequences. However, highly redundant clones are unique to either the RD or RT libraries.

To reduce redundancy, 15744 cDNA clones from the two cDNA libraries were screened with sets of clones known to be redundant within the libraries (Supplementary data 2A shows a background membrane containing 15744 clones, and 2B shows a membrane after hybridizing with a senescence-associated cDNA probe). After a series of screening, 7531 redundant clones (48%) were removed. From the remaining 8213 clones, 2304 clones (931 clones from the RD library and 1373 from the RT library) were randomly selected and sequenced. A total of 2014 sequences with an average insert size of 350 bp were obtained after removing low quality and vector sequences. Sequence analysis revealed that 221 sequences (11%) were singletons. The other 1793 (89%) sequences were assembled into 295 contigs, with each contig having 2–33 overlapping sequences. Thus, after screening out redundant clones, the number of senescence-associated clones was reduced from 20% to 1.7%. Likewise, the abundance of lysine-ketoglutarate reductase and a hypothetic protein were reduced from 9.4% and 12.5% to 1.45% and 1%, respectively. From the original 2014 sequences, a total of 516 unique sequences were obtained. Among them, 281 were from the RD library and 235 were from the RT library. These unique sequences have been submitted to GenBank with accession number DT639225-DT639745 and DW025355-DW025357 and can be accessed at the NCBI EST database (http://www.ncbi.nlm.nih.gov/projects/dbEST).

BlastX and BlastN searches of 516 unique sequences

Because of the methods used to develop the subtractive libraries, non-contiguous sequences could be produced from the same gene, these 516 sequences were thus searched against an EST database of leafy spurge (about 50000 ESTs with 23472 unique sequences) which was developed from a whole plant cDNA library (Unpublished, NCBI EST database). Based on BlastN searches at a cutoff *E*-value of 1E−5, 131 sequences had one or more hits to 104 different genes, and the remaining 385 sequences had no hits. Thus, there are about 489 genes represented among the 516 clones assuming that each of the 385 unmatched sequences represents an individual gene. To determine the number of matches in all protein and nucleotide databases, a BlastX search was performed against protein databases of NCBI at a cutoff value of 1E−5 using the 385 sequences that had no matches with cDNA clones in the leafy spurge EST database. The BlastX search found 222 matches, and the remaining 163 sequences had no matches (Figure 1). A similar BlastX search was performed using the 131 sequences that had one or more hits with cDNA clones in the leafy spurge EST database. Fifty-nine matches were found in this search, while the majority of the sequences (72) had no matches (Figure 1). The results of BlastN leafy spurge cDNA database search and BlastX NR search are provided in the Supplementary data 3.

Furthermore, a BlastN search was performed against the nucleotide database of NCBI. The search results were similar but not identical to the BlastX search. Over half of the sequences (56%) found matches, and most of these matches were plant sequences. Among matched plant sequences, 95 hits were Arabidopsis sequences. A smaller number of matches were

Table 1. A partial list of candidate sequences classified by putative function in the RD library.

Clone ID	Accession #	HIT ID	*E*-value	Molecular function
Hydrolase activity				
RDP3E20	DT639350	At1g02790.1	2.00E−37	Polygalacturonase
RDP7E02	DT639520	At3g51000.1	5.00E−41	Prolyl aminopeptidase
RDP7E09	DT639523	At3g21910.1	5.00E−16	Receptor-like protein kinase-related
Kinase activity				
RDP1H14*	DT639258	At4g23160.1	8.00E−26	Protein kinase
RDP2I24	DT639284	At4g23160.1	1.00E−16	Protein kinase family protein
RDP2N08	DT639306	At4g23180.1	9.00E−29	ATP binding, protein kinase
RDP4N12*	DT639414	At4g23160.1	3.00E−42	Protein kinase
RDP5P12*	DT639476	At4g23160.1	3.00E−10	Protein kinase
Transferase activity				
RDP1I24	DT639261	At3g11480.1	1.00E−17	Methyltransferase
RDP2A13	DT639709	AtCg00170	1.00E−32	RNA polymerase beta′ subunit-2
RDP2B09	DT639715	At1g75910.1	1.00E−27	Acyltransferase
Catalytic activity				
RDP1N23	DT639702	At1g30350.1	8.00E−16	Pectate lyase
RDP2H01	DT639744	At1g62380.1	1.00E−18	Oxidase
RDP3B10	DT639333	At3g13400.1	4.00E−59	Dihydrofolate reductase
RDP7C12	DT639514	At1g20130.1	1.00E−41	Structural constituent of cell wall
RDP8C06	DT639551	At4g33070.1	6.00E−08	Pyruvate decarboxylase
RDP8E08	DT639564	At3g53110.1	9.00E−83	ATP-dependent helicase
RDP8F10	DT639569	At3g13400.1	2.00E−54	Structural constituent of ribosome
RD5F03	DT639660	AtMg00220	2.00E−17	Ubiquinol-cytochrome-*c* reductase
Transcription factor activity				
RDP2A09	DT639708	At1g74840.1	1.00E−16	Transcription factor
DNA or RNA binding				
RDP1D15	DT639234	P10978	6.00E−11	DNA binding protein
RDP1E09*	DT639241	AtMg00710	7.00E−09	Hypothetical protein
RDP2E10	DT639732	AtMg00300	1.00E−07	Hypothetical protein
RDP2O14	DT639316	AtMg00710	1.00E−13	Hypothetical protein
RDP3E13	DT639348	At3g58680.1	6.00E−36	DNA binding
RDP7H12*	DT639537	P10978	6.00E−11	DNA binding
RD5B02*	DT639649	P10978	2.00E−10	DNA binding
RD5E05	DT639660	P10978	8.00E−21	DNA binding protein
Protein binding				
RDP2P20	DT639327	At5g56030.1	3.00E−15	Heat shock protein
Other(ligand) binding				
RDP3I18	DT639364	At5g60390.1	7.00E−09	Calmodulin binding protein
RDP8E05	DT639563	At3g47470.1	2.00E−22	Chlorophyll binding protein
Structural molecular activity				
RDP7F04	DT639526	At5g54270.1	6.00E−72	Structural molecule
Transporter activity				
RDP1A02	DT639225	AtCg00130	3.00E−20	ATP synthase
RDP1M9	DT639695	At4g24120.1	5.00E−50	Oligopeptide transporter
RDP2M06	DT639301	AtCg01110	1.00E−47	NADPH dehydrogenase
RDP2N18	DT639309	At1g50310.1	2.00E−31	Carbohydrate transporter
Molecular function unknown				
RDP2D21	DT639729	P09363	4.00E−52	Unknown
RDP2I23	DT639283	At5g07530.1	9.00E−14	Glycine-rich protein
RDP2K15	DT639294	At5g48575.1	1.00E−11	Hypothetical protein

Table 1. Continued.

Clone ID	Accession #	HIT ID	*E*-value	Molecular function
RDP3C13	DT639338	At5g53820.1	3.00E−07	Similar to ABA-inducible protein
RDP7F03	DT639525	At1g64260.1	3.00E−07	MuDR family transposase
RDP8B11	DT639546	At5g26717.1	3.00E−21	Ribonuclease
Other molecular function				
RDP2O13	DT639315	P26295	8.00E−11	Deoxyribonuclease
RDP3B08	DT639332	At4g22050.1	5.00E−13	Aspartic-type endopeptidase
RDP8C07	DT639552	At2g26020.1	2.00E−16	Plant defensin-fusion protein
RDP8D07	DT639559	At1g61566.1	4.00E−09	Signal transducer

* Represents ESTs obtained from differential screening. Other ESTs that were identified by differential screening but found no matches in the Arabidopsis EST and Swiss-Prot database are RD2A06 (DT639665), RDP1K22 (DT639268), RD4C06 (DT639649), RDP1G20 (DT639256), RDP2O08 (DT639313), RD1A10 (DT639666), RD1B05 (DT639647), RDP1D22 (DT639238), RDP3B14 (DT639334), RDP1C20 (DT639232), RDP3E01 (DT639344), RDP2E08 (DT639731), RD5A11 (DT639667), RD4A12 (DT639668), RD5C06 (DT639651), RDP3B21 (DT639335), RD6H05 (DT639669), RD6B04 (DT639662), and RD1B03 (DT639646).

from the animal kingdom, and these matched sequences were almost exclusive from mouse and human; for instance, 54 hits were mouse sequences and 11 hits were human sequences. Those hits may imply that they were highly conserved genes between animal and plant kingdoms, and since genomic sequences of mouse and human have been completed, more hits were thus likely to be found in these two species. BlastN NT search result is provided in the Supplementary data 3.

Functional annotation of 516 unique sequences

For functional annotation, 516 unique sequences were searched against both the Arabidopsis protein database and Swiss-Prot database at a cutoff *E*-value of 1E−5. The top match was parsed out from the search results, and the identifiers were used to search gene ontology (GO) terms from the GO annotated Arabidopsis database of TIGR/TAIR and database of the European Bioinformatics Institute (EBI). About 185 matches were obtained from the Arabidopsis protein database, and 184 matches were obtained from the Swiss-Prot database. It appears that although Swiss-Prot is non-redundant and cross-referenced to many other databases, it does not contain all the annotated genes in the Arabidopsis protein database. We thus consolidated the matches from these two databases. A total of 226 matches were obtained (131 were from the RT library and 95 were from the RD library) among 516 unique sequences, and the rest of the sequences (56.2%) had no matches from these two sites. For those with no matches, 35.8% of the sequences originated from the RT library and 64.2% from the RD library.

The 226 matched sequences were manually categorized into 12 molecular functional groups based on GO Slim Classification for Plants developed at TAIR (http://www.arabidopsis.org/help/helppages/go_slim_help.jsp) (Figure 2). The hydrolases, kinases, and transferases comprise three distinct functional groups with catalytic activity; whereas the catalytic activity group listed in Figure 2 contains other catalytic enzymes excluding those with hydrolase, kinase, and transferase activities. The annotation results generated a total of 58 RT clones in these four catalytic functional groups, whereas only 25 RD clones were in these four groups. The number of RT clones with catalytic activity was more than two times that observed for RD clones, suggesting that when root buds are released from correlative inhibition, catalytic activity increased. It is noteworthy that metabolic activity has been shown to increase significantly in buds following dormancy release (Gardeal *et al*., 1994). In contrast, the RD library contained more clones with DNA/RNA binding activity (41 sequences, 18%). The significance of these results remains to be identified. The combined number of RD and RT clones in other functional groups were as follows: transcription factor activity (6 sequences, 2.7%), protein binding (6 sequences, 2.7%), ligand binding (9 sequences, 4.0%), structural molecular activity (14 sequences, 6.2%), transporter activity

Table 2. A partial list of candidate sequences classified by putative function in the RT library.

Clone ID	Accession #	HITID	*E*-value	Molecular function
Hydrolase activity				
RTP4F21	DT639391	At3g25050.1	5.00E−81	Hydrolase
RTP4L04	DT639403	At3g52810.1	6.00E−29	Protein serine
RTP5J16	DT639459	At3g62170.1	5.00E−33	Structural constituent of cell wall
RTP5K2	DT639460	At2g47040.1	3.00E−75	Structural constituent of ribosome
RTP9C01	DT639581	At1g69100.1	8.00E−16	Aspartic-type endopeptidase
RTP9E04	DT639591	At3g62170.1	2.00E−07	Pectinesterase
RTP10A03	DT639611	At4g35010.1	3.00E−37	Beta-galactosidase
RTP10G01	DT639632	At2g24560.1	4.00E−19	Carboxylic ester hydrolase
RT2C09	DT639675	At3g14040.1	3.00E−08	Polygalacturonase
Kinase activity				
RTP4N12	DT639414	At4g23160.1	3.00E−42	Kinase protein
RTP4P12	DT639417	At4g37870.1	1.00E−14	Phosphoenolpyruvate carboxykinase
RTP5P12	DT639476	At4g23160.1	3.00E−10	Protein kinase
Transferase activity				
RTP4M11	DT639408	At2g23800.1	4.00E−46	Farnesyltranstransferase
RTP5F18	DT639439	At4g37930.1	1.00E−42	Glycine
RTP6C15*	DT639480	At5g07410.1	2.00E−92	Transferase
RTP6E13	DT639485	At5g20040.2	1.00E−18	tRNA isopentenyltransferase
RTP9E10	DT639595	At1g75930.1	1.00E−09	Acyltransferase
RTP10H12	DT639641	At4g00040.1	2.00E−18	Synthase
RTP11A01	DT639644	P45860	3.00E−06	Phosphotransferase
Catalytic activity				
RTP3O12	DT639372	At5g18620.1	6.00E−19	DNA-dependent ATPase
RTP5F6	DT639438	Q9ZXX8	1.00E−16	Cytochrome-*c* oxidase
RTP5H20*	DT639447	At4g33150.2	9.00E−30	Lysine-ketoglutarate reductase
RTP5I08	DT639451	At3g13390.1	2.00E−53	Multi-copper oxidase
RTP5J10	DT639458	At3g13400.1	6.00E−28	Dihydrofolate reductase activity
RTP5K12	DT639462	Q9I471	9.00E−15	Cobyrinic acid a,c-diamide
RTP10A04	DT639612	At1g54270.1	8.00E−33	ATP-dependent helicase
RTP10B09	DT639620	At5g47000.1	2.00E−28	Peroxidase
RTP10H10*	DT639639	At5g10170.1	2.00E−36	Inositol-3-phosphate synthase
RTP6D13	DT639482	At5g03290.1	4.00E−40	3-Isopropylmalate dehydrogenase
RTP9D05	DT639587	AtMg00580	1.00E−12	NADH dehydrogenase
RT2B06	DT639671	At3g04120.1	1.00E−07	Dehydrogenase
RT6E02*	DT639686	At1g48130.1	2.00E−31	Thioredoxin peroxidase
Transcription factor activity				
RTP3J02	DT639365	At3g28730.1	7.00E−06	Transcription factor
DNA or RNA binding				
RDP2P20	DT639327	At5g56030.1	3.00E−15	Heat shock protein
RTP3I10	DT639362	Q9HB58	4.00E−43	DNA binding polymerase
RTP4J23	DT639401	At1g29990.1	2.00E−23	Prefoldin subunit 6
RTP4N05*	DT639413	At5g60390.1	7.00E−68	Translation elongation factor
RTP5E15	DT639436	Q8K1J6	6.00E−71	ATP binding
RTP6A20	DT639478	At5g20890.1	2.00E−07	T-complex protein
RTP9F05	DT639598	At5g56030.1	9.00E−15	Heat shock protein
Other(ligand) binding				
RTP4C23	DT639383	At5g60390.1	8.00E−68	Calmodulin binding protein
RTP4N5	DT639413	At5g60390.1	7.00E−68	Translation elongation factor
RTP9D06	DT639588	At4g29340.1	3.00E−19	Profilin 3
RT2E04	DT639677	At1g29930.1	5.00E−17	Chlorophyll binding protein

Table 2. Continued.

Clone ID	Accession #	HITID	*E*-value	Molecular function
Structural molecular activity				
RTP4F21	DT639391	NP193044	3.00E−52	Xyloglucasyl transferase
RT2C02	DT639674	At2g43030.1	2.00E−11	Structural constituent of ribosoms
Transporter activity				
RTP3N14	DT639370	Q46877	1.00E−41	Electron transporter binding
RTP4J02	DT639400	At5g56450.1	2.00E−10	Mitochondrial substrate carrier
RTP5I19	DT639454	Q43681	1.00E−06	Lipid binding protein
RTP5L04	DT639464	At2g48020.2	3.00E−42	Carbohydrate transporter
RTP6I04	DT639492	At5g59320.1	2.00E−22	Lipid transfer protein 3
RTP6N13	DT639499	Q9EST3	2.00E−06	Protein transporter
RTP10F07	DT639630	At1g66850.1	5.00E−28	Protease inhibitor protein
RTP10F10	DT639631	At1g50500.1	6.00E−42	Transcription factor
Molecular function unknown				
RTP4G17	DT639395	At3g20220.1	5.00E−33	Auxin-responsive protein
RTP4H14	DT639397	At5g61720.1	1.00E−10	Molecular function unknown
RTP4L08	DT639405	At2g19980.1	9.00E−36	Allergen V5/Tpx-1-related protein
RTP4L21	DT639407	At1g19350.5	2.00E−09	Brassinosteroid signalling regulator
RTP5I20	DT639455	At3g21920.1	7.00E−17	Pollen coat receptor kinase
RTP5M04	DT639467	At3g28790.1	5.00E−12	Molecular function unknown
RTP6E9	DT639484	At4g13560.1	1.00E−12	Embryogenesis protein
RTP6O17	DT639500	At5g07530.1	6.00E−11	Glycine-rich protein
RTP10D09	DT639623	AtMg00810	2.00E−10	Hypothetical protein
RT2A10	DT639670	At5g59845.1	5.00E−36	Gibberellin-regulated protein
Other molecular function				
RTP3H06	DT639358	At1g23220.1	3.00E−10	Dynein light chain protein
RTP3K03	DT639366	At4g24640.1	3.00E−35	Pectinesterase inhibitor
RTP4M18	DT639412	At2g31980.1	1.00E−16	Cysteine protease inhibitor
RTP9G09	DT639605	At5g26717.1	2.00E−22	Ribonuclease
RT2D10	DT639676	P41506	4.00E−06	Defense/immunity protein

*Represents ESTs obtained from differential screening. Other ESTs that were identified by differential screening but found no matches in the Arabidopsis EST and Swiss-Prot database are RT4B04 (DT639688), RT2H08 (DT639689), RT1G02 (DT639690), RT2B06 (DT639671), RT6E08 (DT639691), RT3A12 (DT639692), RT2E11 (DT639693), RT5E10 (DT639694), RTP5O15 (DT639472), RTP6P16 (DT639502), RTP3O19 (DT639373), and RTP5O02 (DT639471).

(18 sequences, 8.0%), molecular function unknown (37 sequences, 16.4%), and other molecular functions (12 sequences, 5.3%). A partial list of candidate sequences classified by putative function is listed in Tables 1 and 2. The comprehensive information is provided as Supplementary data 4.

Macroarray analysis of 516 unique sequences in dormant and growing crown buds

Macroarray analysis was used to determine if any of the 516 genes were differentially expressed in 0 (control), 2 h, 2, and 4 day growth-induced crown buds. Cluster analysis was used to identify coordinately regulated genes (Figure 3). Macroarray analysis indicated that 166 unique sequences showed a general trend of up-regulation ($\log_2$ value > 0, represented by red color) while 151 unique sequences showed a general trend of down-regulation ($\log_2$ value < 0, represented by green color) after 2 h, 2, and 4 d growth induction. The remaining 199 unique sequences showed inconsistent expression patterns after growth induction. The greatest fold-induction ($\log_2$ converted) in anyone of the three time points was 2.42, and the least was −1.08. Twenty-seven percent of the genes showed a significant pattern of differential expression for at least one of the time points based on a 95% confidence interval of *T*-test from 4 independent spots from two biological replicates. Fold-inductions for the majority of unique sequences were similar to the control (∼1) for all three time points. It should be noted that many of the genes are likely derived from rare mRNA

species as supported by the weak radioactive signaling observed in macroarray analysis (data not shown), and thus accurate expression levels among some transcripts may be difficult to obtain.

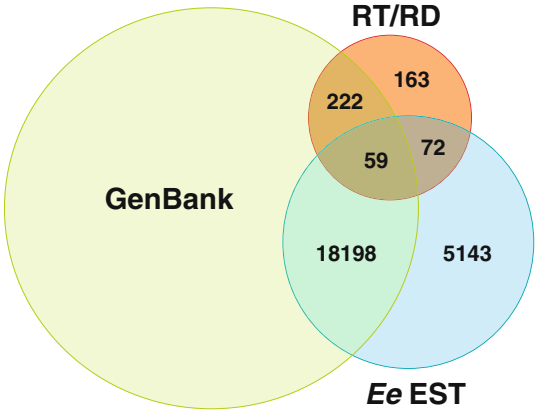

Figure 1. Venn diagram with overlapping clones. The diagram consists of three circles, representing GenBank, 516 unique sequences of the RD and RT cDNA libraries (RD/RT), and 23472 unique sequences in the leafy spurge EST database (*Ee* EST). The number of matched sequences (or ESTs) is placed in the sections where the circles overlap. The diagram serves only as a visual aid, and thus the number represented in each section does not necessarily correspond with the size of that section proportionally.

Histone H3 and *ACC Oxidase* were used as positive controls during macroarray analysis. *Histone H3* transcript levels are known to be up-regulated 2 d after growth induction (Anderson and Horvath, 2001; Horvath *et al.*, 2002). The expression levels of *ACC Oxidase* were up-regulated 2 h after growth induction, went down after 16 h, and cycled back up after 2 d. Normalized data revealed that *Histone H3* and *ACC Oxidase* were up-regulated after growth induction, which are correlated with RT-PCR results (Figure 3).

RT-PCR analysis of gene expression in dormant and growing crown buds

To confirm the macroarray results, randomly selected regions representing unique sequences within a cluster were chosen (Figure 3, designated A, B, and C), and primer pairs were designed for analysis by RT-PCR. The total number of unique sequences in these three areas is 129 (A: 30, B: 55, and C: 44), and 50 primer pairs were designed (A: 15, B: 18, and C: 17). Among these primer pairs, 22 amplified distinct PCR products within 35 cycles (A: 6, B: 8, and C: 8). Figure 4 displays RT-PCR results showing a correlation with macroarray analysis.

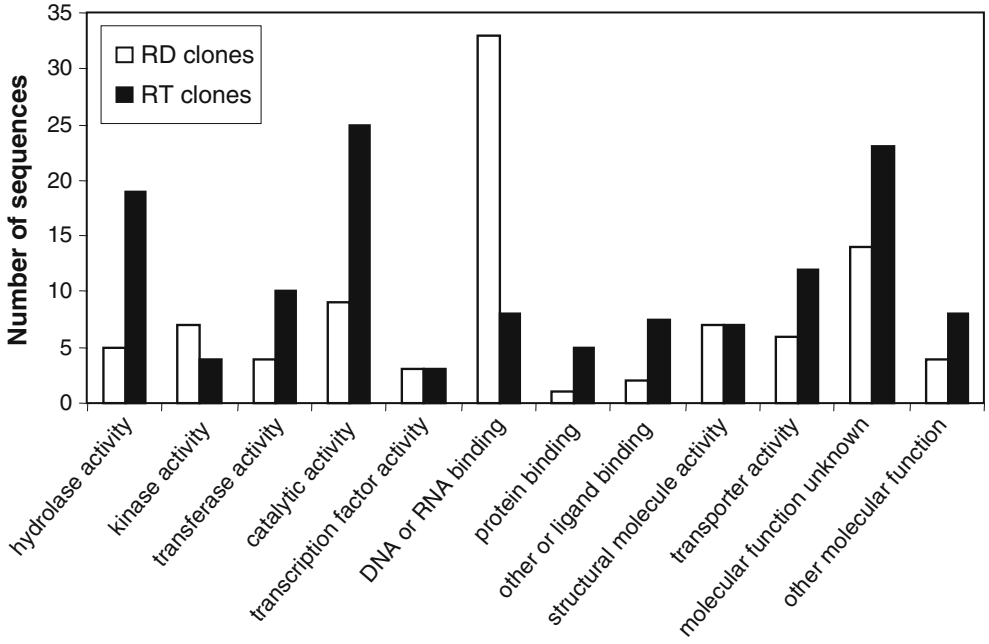

Figure 2. Histogram of molecular functional groups of RD (reverse) and RT (forward) libraries. Matched unique sequences (226) from the subtractive cDNA libraries were categorized into 12 molecular functional groups. White bars represent matched clones from the RD library and black bars represent matched clones from the RT library.

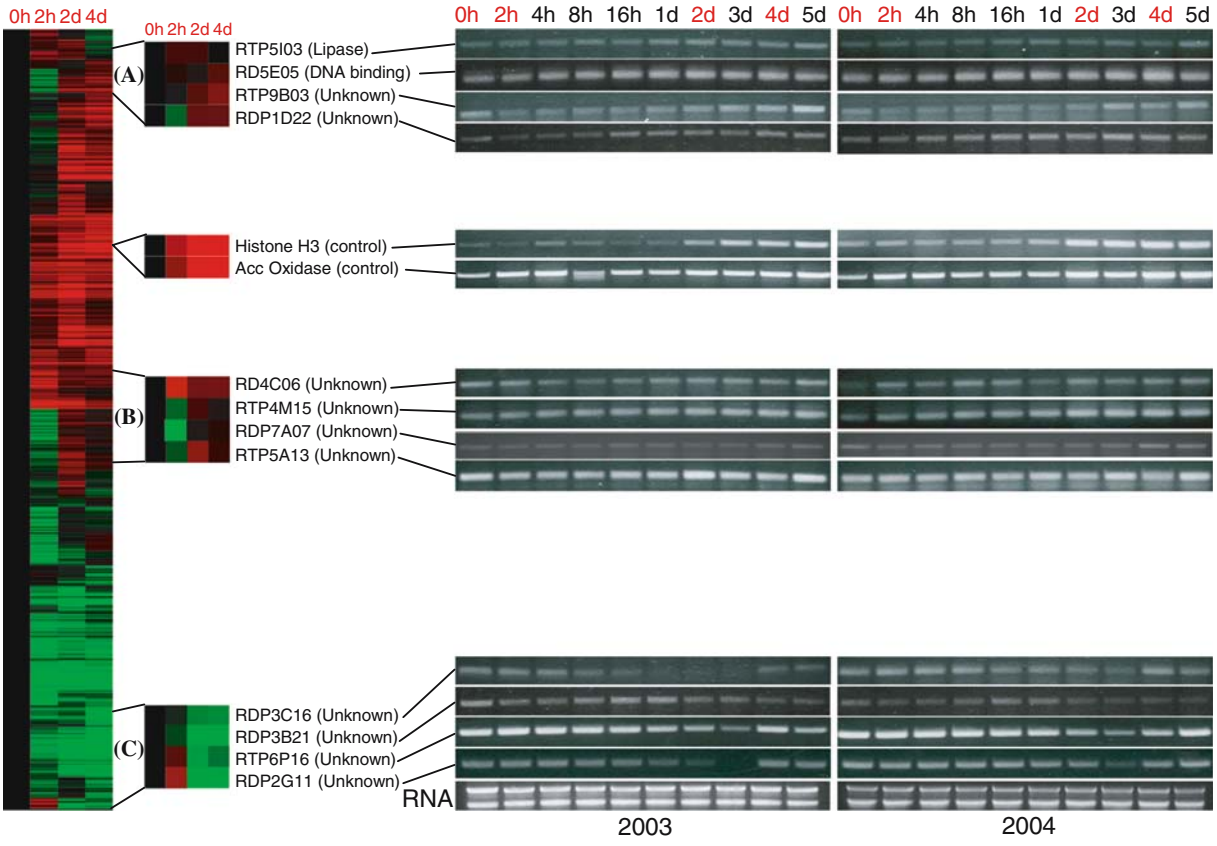

Figure 3. Cluster analysis of macroarray and RT-PCR analysis. Red color indicates up-regulated genes and green color indicates down-regulated genes in cluster analysis. For RT-PCR analysis, time points for replicates (2002 and 2003) are indicated in hours (h) and days (d). RNA gel images are included only as a reference to show that 2 μg of total RNA per sample gives equal banding patterns.

RT-PCR was also used to examine gene expression for 106 additional unique sequences that were situated outside of A, B, and C regions in the cluster. Of the 106 unique sequences, only 26 were amplified by RT-PCR within 35 cycles. RT-PCR results from these 26 and above 22 unique sequences were combined and analyzed. Four different gene expression patterns were identified after grouping similar coordinately regulated ESTs (Figure 4A–D). They include (A) 12 cyclically regulated genes, (B) 8 transiently up-regulated genes, (C) 7 up-regulated genes (Histone H3 is a control), and (D) 11 constitutively expressed genes. A group of 10 irregularly expressed genes were also identified (data not shown). Cyclically regulated genes showed a steady up- or down-regulation of at least 1.5-fold at any one time point following growth induction (Figure 4A). Transiently up-regulated genes showed an increase in transcript levels from as short as 2 h to as long as 4 d after growth induction but an overall decrease in transcript levels was observed by 5 d. Clone RDP3B21, although slightly down-regulated 2 h after growth induction, is grouped with transiently up-regulated genes because its overall expression pattern is closest to this group. Genes showing a continuous increase in transcript levels with at least one time point of 1.5-fold induction are grouped as up-regulated genes (Figure 4C). Unique sequences that had no/minimal changes in transcript levels, or no consistent patterns of gene expression between two biological replicates, were categorized as constitutively expressed (Figure 4D) and irregularly expressed genes (data not shown), respectively. One fact of the RT-PCR results was that both RD and RT clones are shown in those differentially regulated groups (Figure 4A–C).

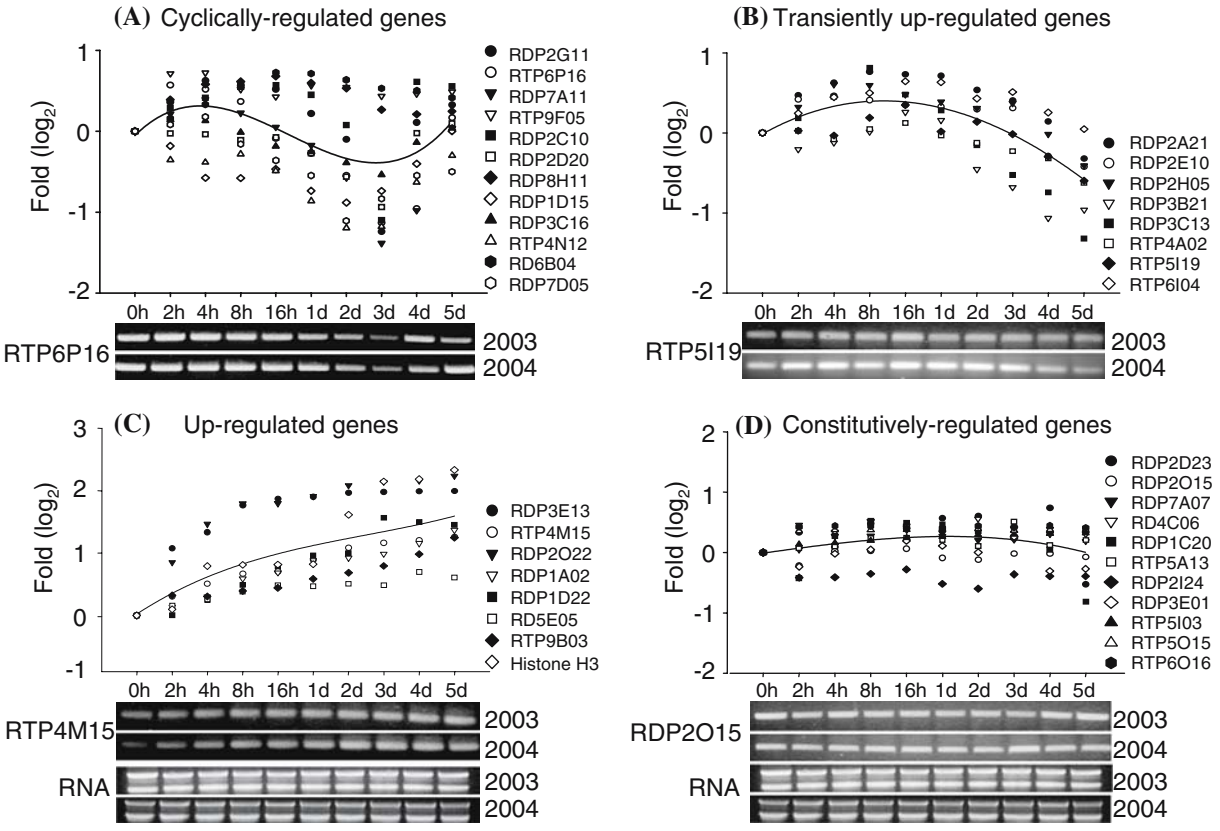

Figure 4. RT-PCR analysis of gene expression in growth-induced, greenhouse-grown crown buds. Time points for replicates (2002 and 2003) are indicated in hours (h) and days (d) on the *X*-axis. Fold inductions were obtained by dividing the value of ethidium bromide pixels of each time point by the 0 h control. Each point (designated with various symbols) is the average fold induction of replicate samples. The average fold value is converted to $\log_2$ (*Y*-axis). Ethidium bromide images under each graph (A, B, C, and D) represent one visual example of the expression pattern. RNA gel images are included only as a reference to show that 2 μg of total RNA per sample gives equal banding patterns.

Seasonal effects on gene expression in field-grown crown buds

Buds that are grown in the field experience dramatically different environmental signals than those that are grown in the greenhouse. To examine if the genes identified from growth-inhibited (para-dormancy) and growth-induced (decapitation) greenhouse-grown buds are influenced by seasonal changes, 14 clones with consistent patterns of differential regulation (Figure 4A–C) were examined during well-defined phases of dormancy using crown buds of field-grown plants. RT-PCR analyses identified two major gene expression patterns based on seasonal effect from July to Feb. (Figure 5A and B). These patterns include 11 seasonally up-regulated genes (Figure 5A) and 3 seasonally down-regulated genes (Figure 5B). These two patterns are very similar as seasonally down-regulated transcripts show a gradual reduction from July through Feb., while the seasonally up-regulated transcripts exhibited some degree of up-regulation between July and Feb. The levels of gene expression for seasonally up-regulated transcripts were generally lowest in Jan. or Feb. and highest from Aug. to Oct.

Discussion

Pre-screening identified non-redundant clones and differentially expressed genes

Differential screening of 1200 randomly selected clones identified only 42 putative differentially

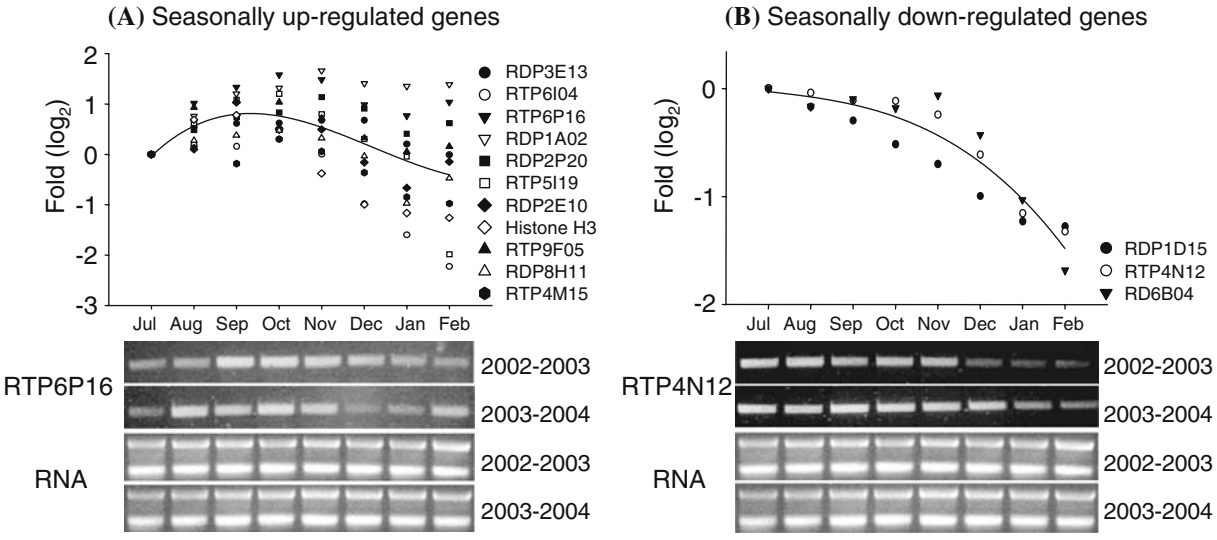

Figure 5. RT-PCR analysis of gene expression in seasonally regulated, field-grown crown buds. Two replicates were harvested July through Feb. 2002–2003 and 2003–2004 and are designated by Jul through Feb. Fold inductions were obtained by dividing the value of ethidium bromide pixels of each month by values for the month of July (Jul.). Each point (designated with various symbols) is the average fold inductions of replicate samples. The average fold value is converted to $\log_2$ (*Y*-axis). RNA gel images are included only as a reference to show that 2 μg of total RNA per sample gives equal banding patterns.

regulated unique sequences (see Tables 1 and 2); mainly attributed to highly redundant clones. High redundancy may be a result of the nature of the samples subtracted against each other or over-expression of these genes in the samples. To ensure that important genes were not overlooked from these two libraries on account of high redundancy, a scrupulous screening approach was applied to reduce redundant clones and increase unique sequences. After screening 15744 clones and sequencing 2304 clones successively, we identified 516 unique sequences from the two libraries. Macroarray and RT-PCR analyses identified many differentially regulated clones whose sequences were unrelated to the 43 clones obtained by differential screening. For example, RT-PCR analyses on growth induced samples identified 24 differentially regulated clones (Figure 4A–C). Among them only four clones, RDP3B21, RD6B04, RTP4N12, and RTP6P16 were identified by the differential screening method. These results indicated that performing differential screening may be an effort-saving approach to obtain differentially regulated genes; nonetheless, differential screening would in fact overlook many differentially regulated genes.

Most genes were expressed at low levels

Blast searches revealed that >50% of the 516 unique sequences had no matches in Arabidopsis EST and Swiss-Prot databases (Figure 2). Additional searches were performed against an EST database of leafy spurge which contained approximately 50000 ESTs (representing 23472 unique sequences) indicated that 385 sequences had no matches (Figure 1). When performing BlastX and BlastN searches against all organisms in NCBI, almost 50% of the sequences had no matches (BlastX = 46%; BlastN = 44%) (Figure 1 and Supplementary data 3). In contrast, about 78% of the 23472 unique sequences in leafy spurge EST database found matches (Figure 1). The combined result of these searches indicates that the subtraction selected for rare mRNA species. In fact, a high number of rare mRNA species may be reflected by the results of macroarray analyses where radioactive signals in many hybridized clones were low. Moreover, when performing RT-PCR analysis, primers were designed from over 100 unique sequences, and only 1/3 (47/128) of these primers generated PCR products within 35 cycles. For those primers that did not generate a visible band within

35 cycles, designing new primer pairs did not improve results. Secondary structures in the mRNA usually hamper PCR reactions; yet rare mRNA species also can be the cause of setbacks in PCR reactions. Thus, subtractive hybridization appeared to be a useful tool for isolating rare mRNA species that may be differentially regulated.

The change in transcript levels of differentially expressed genes including cyclically, transiently up-, and up-regulated genes were not vivid (Figure 4A–C). These results could be due to control and growth-induced samples being harvested in a relatively short time point (0 h to 5 d after growth induction). Phenotypically, growth-induced buds are difficult to distinguish from control buds within 3 d after growth induction. In addition, growth induction usually causes 1/3 or less of buds to grow. The remaining 2/3 of buds would either grow very slow or remain visually unchanged. Since the growth of crown and root buds of leafy spurge cannot be induced synchronously, the vividness of gene expression in both macroarray and RT-PCR analyses is likely diluted. In this study, we also see that both RD and RT clones are shown in those differentially regulated groups (Figure 4A–C); cyclic and/or transient-up regulation on gene expression may be one explanation for this result.

Gene expression in growth-induced and seasonally regulated crown buds

In growth-induced crown buds, 4 major gene expression patterns were classified after analyzing RT-PCR results from 47 cDNA clones. Among them, a cyclic pattern appeared to be most prevalent (Figure 4A). One unique feature of these cyclically regulated transcripts was that they showed a steady decrease in expression levels up to day 3 after growth induction. At day 4, transcript levels were suddenly up-regulated. This phenomenon is interesting since dramatic changes in morphology, namely, from buds to shoots, can be visually observed on the 4th day after growth induction. These genes are thus likely to be growth-related. Unique sequences designated as transiently up-, and up-regulated genes (Figure 4B–C) also displayed ordered patterns of transcript levels during growth and thus may also be growth-related. Many of these unique sequences were also used to examine seasonal effects on the expression of these genes in field-grown leafy spurge.

Two major transcript patterns (seasonally up- and seasonally down-regulated) were identified from July to Feb. in field-grown crown buds. Both patterns are similar in that they all show a dramatic down-regulation after breaking of endo-dormancy and during the winter (Dec. through Feb.) where growth is controlled by eco-dormancy. The levels of expression observed for the major, seasonally up-regulated transcripts were highest from Aug through Oct., correlating with the dramatic changes in physiological status of these buds during the transition from para- to endo-dormancy, and bud enlargement during the period of endo-dormancy. Interestingly, in field-grown plants, sucrose levels increased during the transition from para- to endo-dormancy (Anderson *et al*., 2005), and sucrose has also been shown to inhibit root bud growth in greenhouse-grown plants (Chao *et al*., 2006). Since the expression of *Histone H3* remained high during the transition from para- to endo-dormancy, sucrose levels appear to have no direct effect on this marker gene for S-phase progression. Thus, seasonally up-regulated genes observed in this study are similar to the regulation of *Histone H3*, which is growth-related but not sucrose-regulated.

Based on sequence information, the potential function of some unique sequences may be postulated. For example, the deduced amino acid sequence of RTP6P16 is very similar to a snow pea protein (AB049723) whose transcript is down-regulated during senescence (Pariasca *et al*., 2001). RTP6P16 has a high sequence identify (86%) with a tobacco cytochrome P-450-like protein (T02995). Sugiura et al. (1996) demonstrated that this tobacco P-450-like protein had monooxygenase activity which is related to xenobiotic metabolism. Cytochrome P450 was also shown to regulate auxin production and played a role in apical dominance (Bak *et al*., 2001). The transcript of RTP6P16 showed trivial change before 24 h after growth induction in crown buds of greenhouse-grown plants. A vivid down-regulation was observed from day 1 to day 3; however, on the 4th day after growth induction, it was up-regulated. In crown buds of field-grown plants, RTP6P16 was up-regulated from Aug. through Oct. and down-regulated afterwards. The expression pattern of this gene is consistent with a role in senescence.

Another sequence, RTP5I19, encodes a putative lipid transfer protein. It was up-regulated prior to the 3rd day after growth induction and down-regulated on the 3rd or 4th day in crown buds of greenhouse-grown plants. In crown buds of field-grown plants, RTP5I19 was up-regulated from Aug. through Nov. Lipid mobilization was shown to affect seed dormancy and growth (Footitt *et al*., 2002). These two proteins may thus be involved in cell growth and/or development/maintaining of para- and endo-dormancy.

Finally, the patterns of gene expression in growth-induced and seasonally regulated crown buds have identified numerous coordinately regulated genes. Conservation of *cis*-acting sequences within coordinately regulated genes has been proven to be a viable means to identify such sequences and provides starting points for identifying the trans-acting elements that interact with them. Studying the mechanisms that regulate these genes could provide insight on coordination of cellular and molecular events during dormancy and growth. Identifying upstream regulatory genes will provide insight into the regulatory mechanisms governing the coordinate expression of these genes and could provide new target sites for weed management.

Acknowledgments

The authors acknowledge Wayne Sargent, USDA-ARS, Fargo, ND, for his technical assistance and Dr. Mark West, USDA-ARS, Fort Collins, CO, for assistance in statistical analysis. Funding for this work was provided by USDA-National Research Initiative (2003-35320-13761) and the USDA-ARS.

References

Anderson, J.V., Chao, W.S. and Horvath, D.P. 2001. A current review on the regulation of dormancy in vegetative buds. Weed Sci. 49: 581–589.

Anderson, J.V. and Horvath, D.P. 2001. Random sequencing of cDNAs and identification of mRNAs. Weed Sci. 50: 227–231.

Anderson, J.V., Gesch, R.W., Jia, Y., Chao, W.S. and Horvath, D.P. 2005. Seasonal shifts in dormancy status, carbohydrate metabolism, and related gene expression in crown buds of leafy spurge. Plant Cell Environ. 28: 1567–1578.

Bak, S., Tax, F.E., Feldmann, K.A., Galbraith, D.W. and Feyereisen, R. 2001. CYP83B1, a cytochrome P450 at the metabolic branch point in auxin and indole glucosinolate biosynthesis in *Arabidopsis*. Plant Cell 13: 101–111.

Bassani, M., Neumann, P.M. and Gepstein, S. 2004. Differential expression profiles of growth-related genes in the elongation zone of maize primary roots. Plant Mol. Biol. 56: 367–380.

CAB International 2004. *Euphorbia esula* [original text by W. Chao and J.V. Anderson]. In: Crop Protection Compendium, 2004 edition. CAB International, Wallingford, UK [CD-ROM].

Chang, S., Puryear, J. and Cairney, J. 1993. A simple and efficient method for isolating RNA from pine trees. Plant Mol. Biol. Rep. 11: 113–116.

Chao, W.S., Serpe, M.D., Anderson, J.V., Gesch, R.W. and Horvath, D.P., 2006. Sugars, hormones, and environment affect the dormancy status in underground adventitious buds of leafy spurge (*Euphorbia esula*). Weed Sci. 54: 59–68.

Coupland, R.T., Selleck, G.W. and Alex, J.F. 1955. Distribution of vegetative buds on the underground parts of leafy spurge (*Euphorbia esula* L.). Can. J. Agric. Sci. 35: 161–167.

Diatchenko, L., Lau, Y.F., Campbell, A.P., Chenchik, A., Moqadam, F., Huang, B., Lukyanov, S., Lukyanov, K., Gurskaya, N., Sverdlov, E.D. and Siebert, P.D. 1996. Suppression subtractive hybridization: a method for generating differentially regulated or tissue-specific cDNA probes and libraries. Proc. Natl. Acad. Sci. USA 93: 6025–6030.

Footitt, S., Slocombe, S.P., Larner, V., Kurup, S., Wu, Y., Larson, T., Graham, I., Baker, A. and Holdsworth, M. 2002. Control of germination and lipid mobilization by *COMATOSE*, the *Arabidopsis* homologue of human ALDP. EMBO J. 21: 2912–2922.

Frewen, B.E., Chen, T.H.H., Howe, G.T., Davis, J., Rohde, A., Boerjan, W. and Bradshaw, H.D. Jr. 2000. Quantitative trait loci and candidate gene mapping of bud set and bud flush in populus. Genetics 154: 837–845.

Freyre, R., Warnke, S., Sosinski, B. and Souches, D.S. 1994. Quantitative trait locus analysis of tuber dormancy in diploid potato (*Solanum* spp). Theor. Appl. Genet. 89: 474–480.

Gardeal, A.A., Moreno, Y.M., Azarenko, A.N., Lombard, P.B., Daley, L.S. and Criddle, R.S. 1994. Changes in metabolic properties of grape buds during development. J. Am. Soc. Hort. Sci. 119: 756–760.

Harvey, S.J. and Nowierski, R.M. 1988. Release of postsenescent dormancy in leafy spurge (*Euphorbia esula* L.) by chilling. Weed Sci. 36: 784–786.

Horvath, D.P. 1998. The role of specific plant organs and polar auxin transport in correlative inhibition of leafy spurge (*Euphorbia esula* L.) root buds. Can. J. Bot. 76: 1227–1232.

Horvath, D.P. 1999. Role of mature leaves in inhibition of root bud growth in *Euphorbia esula* L. Weed Sci. 47: 544–550.

Horvath, D.P. and Anderson, J.V. 2002. A molecular approach to understanding root bud dormancy in leafy spurge. Weed Sci. 50: 227–231.

Horvath, D.P., Chao, W.S. and Anderson, J.V. 2002. Molecular analysis of signals controlling dormancy and growth in underground adventitious buds of leafy spurge (*Euphorbia esula* L.). Plant Physiol. 128: 1439–1446.

Horvath, D.P., Anderson, J.V., Chao, W.S. and Foley, M.E. 2003. Knowing when to grow: signals regulating bud dormancy. Trends Plant Sci. 8: 534–540.

Horvath, D.P., Anderson, J.V., Jia, Y. and Chao, W.S. 2005. Cloning, characterization and expression of growth regulator CYCLIN D3–2 in Leafy Spurge (*Euphorbia esula*). Weed Sci. 53: 431–437.

Lazo, G.R., Lui, N., Gu, Y.Q., Kong, X., Coleman-Derr, D. and Anderson, O.D. 2005. Hybsweeper: a resource for detecting high-density plate gridding coordinates. BioTechniques 39: 320–324.

McIntyre, G.I. 1972. Developmental studies on *Euphorbia esula* L. The influence of the nitrogen supply on the correlative inhibition of root bud activity. Can. J. Bot. 50: 949–956.

Nissen, S.J. and Foley, M.E. 1987a. Correlative inhibition and dormancy in root buds of leafy spurge (*Euphorbia esula* L.). Weed Sci. 35: 155–159.

Nissen, S.J. and Foley, M.E. 1987b. *Euphorbia esula* L. root and root bud indole-3-acetic acid levels at three phenologic stages. Plant Physiol. 84: 287–290.

Pariasca, J.A.T., Sunaga, A., Miyazaki, T., Hisaka, H., Sonoda, M., Nakagawa, H. and Sato, T. 2001. Cloning of cDNAs encoding senescence-associated genes, Acc synthase and Acc oxidase from stored snow pea pods (*Pisum sativum* L. var Saccharatum) and their expression during pod storage. Postharvest Biol. Technol. 22: 239–247.

Paterson, A.H., Scherz, K.F., Lin, Y.R., Liu, S.C. and Chang, Y.L. 1995. The weediness of wild plants: molecular analysis of genes influencing dispersal and persistence of johnsongrass, *Sorghum halepense* (L.) Pers. Proc. Natl. Acad. Sci. USA 92: 6127–6131.

Sambrook, J., Fritsch, E.F. and Maniatis, T. 1989. Molecular Cloning – A Laboratory Manual. Cold Spring Harbor Laboratory Press, Cold Spring Harbor, NY.

Sebastiani, P., Gussoni, E., Kohane, I.S. and Ramoni, M.F. 2003. Statistical challenges in functional genomics. Statistical Sci. 18: 33–70.

Šimko, I., McMurry, S., Yang, H.M., Manschot, A., Davies, P.J. and Ewing, E.E. 1997. Evidence from polygene mapping for a causal relationship between potato tuber dormancy and abscisic acid content. Plant Physiol. 115: 1453–1459.

Sugiura, M., Sakaki, T., Yabusaki, Y. and Ohkawa, H. 1996. Cloning and expression in *Escherichia coli* and *Saccharomyces cerevisiae* of a novel tobacco cytochrome P-450-like cDNA. Biochim. Biophys. Acta 1308: 231–240.

Van den Berg, J.H., Ewing, E.E., Plaisted, R.L., McMurry, S. and Bonierbale, M.W. 1996. QTL analysis of potato tuber dormancy. Theor. Appl. Genet. 93: 317–324.

Zheng, J., Zhao, J., Tao, Y., Wang, J., Liu, Y., Fu, J., Jin, Y., Gao, P., Zhang, J., Bai, Y. and Wang, G. 2004. Isolation and analysis of water stress induced genes in maize seedlings by subtractive PCR and cDNA macroarray. Plant Mol. Biol. 55: 807–823.